IOPscience iopscience.iop.org

Home Search Collections Journals About Contact us My IOPscience

On the stability of the mean-field spin glass broken phase under non-Hamiltonian perturbations

This article has been downloaded from IOPscience. Please scroll down to see the full text article.

1997 J. Phys. A: Math. Gen. 30 4489

(http://iopscience.iop.org/0305-4470/30/13/007)

View the table of contents for this issue, or go to the journal homepage for more

Download details:
IP Address: 171.66.16.72
The article was downloaded on 02/06/2010 at 04:24

Please note that terms and conditions apply.

J. Phys. A: Math. Gen. **30** (1997) 4489–4511. Printed in the UK PII: S0305-4470(97)80126-6

On the stability of the mean-field spin glass broken phase under non-Hamiltonian perturbations*

G Iori†§ and E Marinari‡‖

† Dipartimento di Fisica and Infn, Università di Roma *La Sapienza*, P A Moro 2, 00185 Roma, Italy

‡ Dipartimento di Fisica and Infn, Università di Cagliari, Via Ospedale 72, 09100 Cagliari, Italy

Received 2 December 1996

Abstract. We study the dynamics of the SK model modified by a small non-Hamiltonian perturbation. We study aging, and we find that on the timescales investigated by our numerical simulations it survives a small perturbation (and is destroyed by a large one). If we assume that we are observing a transient behaviour, the scaling of correlation times versus the asymmetry strength is not compatible with the one expected for the spherical model. We discuss the slow power law decay of observable quantities to equilibrium, and we show that for small perturbations power-like decay is preserved. We also discuss the asymptotically large time region on small lattices.

1. Introduction

The non-Hamiltonian generalization of the dynamics of the Sherrington Kirkpatrick (SK) model is an interesting problem. The main question is if the complex dynamical behaviour of the SK model (implying aging, slow power-like decays and related effects) is stable under a small non-Hamiltonian perturbation.

The question is very relevant, since in many physical systems we would expect the presence of non-Hamiltonian effects: would a replica broken dynamics survive such small effects? We believe that this is an important question, and we will later give indications towards a positive answer.

The problem has been analysed in detail in many papers, but definite conclusions are difficult to reach. Crisanti and Sompolinsky [1, 2] have studied a simplified version of the mean-field, spherical model (see later in the text), and have shown that for this model a small perturbation is enough to destabilize the glassy phase. For large asymmetry two other studies agree with this conclusion [3, 4].

The fully asymmetric model has been studied in detail in [1, 4–6]. The $T = 0$ case has been discussed in [7–10]. Techniques such as damage spreading have also been used [11] (by reaching conclusions about the possible survival of a complex behaviour similar to the ones we reach here). The p-spin model (with $p > 2$) has also been studied recently [12].

Here we will try to distinguish two different aspects of the non-Hamiltonian generalization of the SK model. On the one hand we will discuss its dynamical behaviour, by

* In memory of our friend Giovanni Paladin.

§ E-mail address: iorig@roma1.infn.it

‖ E-mail address: marinari@ca.infn.it

0305-4470/97/134489+23$19.50 © 1997 IOP Publishing Ltd

focusing on aging-like effects. On the other hand we will look at the long time *equilibrium* limit of the model, on smaller lattices. We will compare our numerical results with the spherical model results, and will discuss the possibility that their main features could also be valid for the SK model.

In section 2 we remind the reader of some theoretical results. In section 3 we give the definitions we will need later. In section 4 we discuss aging-like effects. In section 5 we show slow, power law decays. These two sections deal with dynamic behaviours: we use large lattices and we stay far from equilibrium. In section 6 we discuss long equilibrium runs, on small lattices and in section 7 we draw our conclusions.

2. Theory

Even though, as we have said, a large amount of work has been devoted to the study of non-Hamiltonian disordered models [1–12], the main results concerning the general case of the finite T spherical spin model with non-symmetric couplings have already been obtained in [1], while many of the other works deal with special cases such as the $T = 0$ dynamics or the fully asymmetric case. Here we are interested in the finite T dynamics of a SK model (as opposed to the spherical model) that is perturbed by a small, non-Hamiltonian term, and as we will discuss not much is known about this case.

In order to make the situation clearer we shall give a brief outline of the results obtained in [1, 2], that are based on the dynamic mean-field formalism of [13].

The generalization of the usual spin glass dynamics is done by using the couplings

$$J_{i,j} = J^{\mathrm{S}}_{i,j} + k J^{\mathrm{AS}}_{i,j} \tag{1}$$

where $J^{\mathrm{S}}_{i,j} = J^{\mathrm{S}}_{j,i}$, and $J^{\mathrm{AS}}_{i,j} = -J^{\mathrm{AS}}_{j,i}$ (with a definition of the asymmetry parameter k slightly different from the ϵ we will use later, see (17)). Both J types have zero average over the disorder and

$$\overline{J^{\mathrm{S}^2}} = \overline{J^{\mathrm{AS}^2}} = \frac{J^2}{N}\frac{1}{1+k^2} \tag{2}$$

where the overline indicates the average over the disorder and brackets will denote the thermal average. One writes the non-Hamiltonian generalization of the *soft spin* ($\sigma_i \in [-\infty, +\infty]$) SK mean-field model, whose dynamics is governed by the Langevin equation

$$\Gamma_0^{-1}\frac{\partial}{\partial t}\sigma_i(t) = -r_0\sigma_i(t) - \frac{\delta V(\sigma_i(t))}{\delta\sigma_i(t)} + \sum_j J_{i,j}\sigma_j(t) + h_i(t) + \xi_i(t) \tag{3}$$

where J contains the two contributions of (1). The potential controls fluctuations in the amplitude of the soft spins $\sigma_i(t)$, h is a local external field, and ξ is a white noise, with

$$\langle \xi_i(t)\xi_j(t')\rangle = \frac{2T}{\Gamma_0}\delta(t-t')\delta_{i,j} \tag{4}$$

where T represents temperature (for this model, where *a priori* one cannot expect to reach thermal equilibrium). The autocorrelation

$$C(t) = \overline{\langle \sigma_i(t+t')\sigma_i(t')\rangle} \tag{5}$$

and the response function

$$\left.\frac{\delta\overline{\langle\sigma_i(t+t')\rangle}}{\delta h_i(t')}\right|_{h=0}, t \geqslant 0 \tag{6}$$

are the main dynamical observable quantities. The static susceptibility χ is defined as

$$\chi \equiv \int_{-\infty}^{+\infty} \mathrm{d}t\, G(t). \tag{7}$$

After taking the $N \to \infty$ limit one can use the approach of [13] and write the mean-field equations of motion

$$\Gamma_0^{-1} \frac{\partial}{\partial t}\sigma_i(t) = -r_0\sigma_i(t) - \frac{\delta V(\sigma_i(t))}{\delta \sigma_i(t)} + h_i(t) + \phi_i(t) + J^2 \frac{1-k^2}{1+k^2} \int_{-\infty}^{t} \mathrm{d}t'\, G(t-t')\sigma_i(t') \tag{8}$$

where $\phi_i(t)$ is a Gaussian variable with zero mean and variance

$$\langle \phi_i(t)\phi_i(t)\rangle = \frac{2T}{\Gamma_0}\delta(t-t') + J^2 C(t-t'). \tag{9}$$

The detailed treatment done in [13] cannot be repeated in the case $k \neq 0$, where things become too complicated. In contrast, the spherical model, or p-spin model (here with $p = 2$), can still be treated in a satisfactory way. The spherical model (that can be seen as a mean field of the mean field, or, simply, as a different model from SK) can be defined through the Langevin equation

$$\Gamma_0^{-1} \frac{\partial}{\partial t}\sigma_i(t) = -r\sigma_i(t) + \sum_j J_{i,j}\sigma_j(t) + h_i(t) + \xi_i(t) \tag{10}$$

where we have only kept the quadratic part of the potential (that had already been extracted in the r-term in (3)), and where now the parameter r is not a free parameter but such that

$$\frac{1}{N}\sum_i \sigma_i(t)^2 = 1. \tag{11}$$

In this approach one easily checks that for the symmetric model, $k = 0$, $\chi = 1/T$ for $T > T_g$ (where T_g is the first temperature where q takes a non-zero expectation value). There is a spin glass transition at $T_g = 1$, and $\chi = 1$ for $T \leqslant T_g$.

For the asymmetric case $k \neq 0$ at finite T one finds that there cannot be any transition (we will not discuss what happens at $T = 0$ here, since in our numerical simulations we always investigate the system at finite T): $q = 0$ for all $T > 0$. The reason is that $G(\omega)$ is singular when $\chi^2 = 1 - k^2/1 + k^2$, while $C(\omega)$ is singular at $\chi = 1$. That implies that χ stops at 1 in order to not violate finiteness of correlation functions.

Finally, we recall that [1] finds that for small k the correlation time τ diverges like

$$\tau \simeq k^{-6}. \tag{12}$$

The way of reasoning, that we explained two paragraphs ago, would also suggest (as found by Hertz *et al* [3]) that the same thing happens in the full SK mean-field model. But in the case of the SK model this is only a qualitative argument: for example replica symmetry breaking could change things: for example Crisanti and Sompolinsky [1] discuss the possible appearance of a hierarchical distribution of large correlation times, and of a slow component not only in $C(\omega)$ but also in $G(\omega)$. In the rest of this paper we will study the case of the full fledged SK model, in the regime where the Parisi solution characterizes the symmetric model.

Cugliandolo *et al* [12] found that the result of [1] is also valid when one does not assume *a priori* time translational invariance [14], for a p-spin model with $p > 2$. They are interested in the behaviour of the p-spin model for $p > 2$ (that is non-marginal, and in some sense more general than the SK model). They also find that (for $N < \infty$) in the

p-spin model there are deep stable states that show a complex dynamical behaviour even in the non-symmetric case.

At last we note that Parisi [4] proposed to use spin glass systems with non-Hamiltonian perturbation as a way of building memories that can be confused, and he suggested that the asymmetry can be crucial for the process of learning.

3. Definitions

We will give here all the definitions that are relevant for the model discussed in this paper. We consider an infinite range model, based on spin variables $\sigma_i = \pm 1$, where $i = 1, \ldots, N$ labels site. The couplings $J_{i,j} = \pm 1/\sqrt{N}$ with uniform probability (both the symmetric couplings $J_{i,j}^{(\mathrm{S})}$ and the non-symmetric ones $J_{i,j}^{(\mathrm{NS})}$). The usual SK version of the mean-field spin glass is defined by a probability distribution for the spin variables built over a Hamiltonian

$$P(\{\sigma\}) \simeq \mathrm{e}^{-\beta H} = \mathrm{e}^{\beta \sum_i \sigma_i \sum_j J_{i,j}^{(\mathrm{S})} \sigma_j} \equiv \mathrm{e}^{\sum_i \sigma_i F_i} \tag{13}$$

where $J_{i,j}^{(\mathrm{S})}$ are the usual quenched, symmetric random variables, with $J_{i,j}^{(\mathrm{S})} = J_{j,i}^{(\mathrm{S})}$.

We run a local dynamics, usually known as *heat bath*: each spin σ_i is in turn equilibrated with the field given by the other spins. The probability for the new spin σ_i to be $+1$ after the update is

$$P(\sigma_i = +1) = \frac{\mathrm{e}^{F_i}}{\mathrm{e}^{F_i} + \mathrm{e}^{-F_i}}. \tag{14}$$

We measure the expectation value (thermal and over the disorder) of the internal energy at time t

$$E(t) = \frac{1}{N} \overline{\left\langle \sum_i \sigma_i F_i \right\rangle}. \tag{15}$$

We always follow two copies (α and β) of the system in a given quenched realization of the couplings, and we compute the overlap

$$q(t) \equiv \frac{1}{N} \left\langle \sum_i \sigma_i^{(\alpha)} \sigma_i^{(\beta)} \right\rangle. \tag{16}$$

In the non-Hamiltonian case one updates the spins under the field

$$F_i \equiv \beta \frac{1}{\sqrt{1 - 2\epsilon + 2\epsilon^2}} \sum_j [(1-\epsilon) J_{ij}^{(\mathrm{S})} + \epsilon J_{ij}^{(\mathrm{NS})}] \sigma_j \equiv F_i^{(\mathrm{S})} + F_i^{(\mathrm{NS})} \tag{17}$$

where now $J_{i,j}^{(\mathrm{NS})}$ is drawn independently from $J_{j,i}^{(\mathrm{NS})}$, and we have called $F_i^{(\mathrm{S})}$ the part of F_i proportional to $J^{(\mathrm{S})}$ and $F_i^{(\mathrm{NS})}$ the part proportional to $J^{(\mathrm{NS})}$. This is the model we are going to analyse. ϵ and k of [1] have the same scaling behaviour when they are small, and play the same role.

In the case of the non-Hamiltonian extension of the dynamics we also measure separately the symmetric and the non-symmetric contributions to the energy, i.e.

$$E^{(\mathrm{S})}(t) = \frac{1}{N} \overline{\left\langle \sum_i \sigma_i F_i^{(\mathrm{S})} \right\rangle} \qquad E^{(\mathrm{NS})}(t) = \frac{1}{N} \overline{\left\langle \sum_i \sigma_i F_i^{(\mathrm{NS})} \right\rangle}. \tag{18}$$

We define the time-dependent correlation function

$$c(t_w, t_w + t) \equiv \frac{1}{N} \sum_{i=1}^{N} \overline{\langle \sigma_i(t_w) \sigma_i(t_w + t) \rangle}. \tag{19}$$

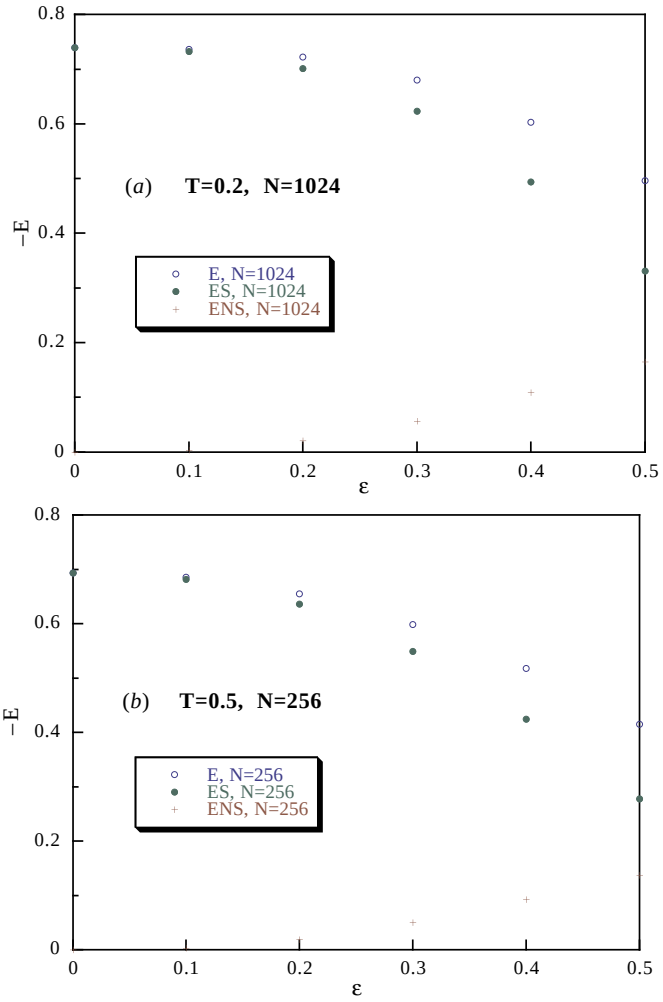

Figure 1. Expectation values of the total energy operator, of the symmetric part and of the non-symmetric part as a function of the asymmetry parameter ϵ.

(This figure can be viewed in colour in the electronic version of the article; see `http://www.iop.org`)

We measure the correlation functions $c(t_w, t_w + t)$ for all t_w and t of the form 2^n, with n being an integer. All the data analysis we will describe in the following will be based on the knowledge of the $c(t_w, t_w + t)$ at these times.

To try to quantify the effect of a given ϵ value we plot in figure 1 the expectation value of the total energy operator (empty dots), of its symmetric part (full dots) and of the non-symmetric part (plus symbols). Error bars are smaller than the symbols. There is an important difference between distinguishing data at $T = 0.2$ and those at $T = 0.5$ (all taken from averages over the last two thirds of our total Monte Carlo sweeps). Data at $T = 0.5$ on a small lattice, $N = 256$, are at equilibrium, in the sense that their average does not depend on time anymore. In contrast, data at $T = 0.2$ are for some ϵ values out of equilibrium (see fits later on): but this is a small effect, not relevant for the present

purpose. At $\epsilon = 0.0$ obviously the total energy coincides with the symmetric contribution, while the non-symmetric part is zero by construction. As ϵ becomes different from zero the non-symmetric part acquires a non-zero expectation over the dynamics: at $\epsilon = 0.1$ it remains very small, while at $\epsilon = 0.5$ it is of the same order of magnitude as the symmetric contribution. The $T = 0.2$ and $T = 0.5$ cases look, from figure 1 to be very similar.

The computer runs discussed in this paper have taken a few months to complete even when using computers of the class of a Pentium 133 or of a 3000/300 Digital α Unix workstation.

4. Aging

First we will try to understand the dynamical behaviour of such systems, by studying aging phenomena [15]. We will start by looking, as a reference point, at the usual Hamiltonian SK model.

We will look as usual at the time-dependent correlation function $c(t_w, t_w + t)$. Our *dynamical* runs (where we do not try to reach thermal equilibrium) have been done at $T = 0.2$ (for the SK model, $\epsilon = 0$, $T_c = 1$). We have studied systems with different numbers of sites, up to $N = 1024$ (the case we will discuss later). For $N = 1024$ we have 20 samples for each different ϵ value.

In figure 2 we plot $c(t_w, t_w + t)$ as a function of t, for different values of t_w (lower curves depict smaller t_w values). Here $N = 1024$, $\epsilon = 0$ (i.e. the Hamiltonian case of the usual SK model). Error bars come from sample-to-sample fluctuations. The system starts from a disordered configuration, and we let it evolve. The fact that the correlation function is not time-translational invariant is very clear: $c(t_w, t_w + t)$ is not only a function of t. For

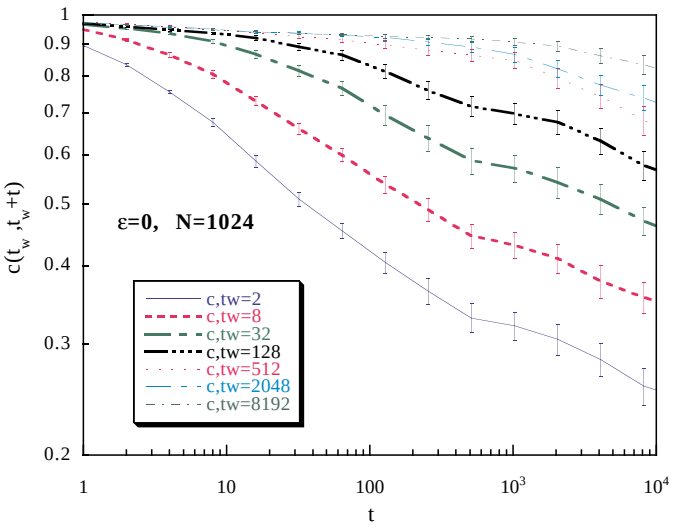

Figure 2. The spin–spin time-dependent correlation functions $c(t_w, t_w + t)$ as a function of t, for different values of t_w (lower curves for smaller t_w values). There were 20 samples, $N = 1024$, $\epsilon = 0$ (i.e. the Hamiltonian case of the usual SK model). Error bars are from sample-to-sample fluctuations. This plot is on a log–log scale.

(This figure can be viewed in colour in the electronic version of the article; see `http://www.iop.org`)

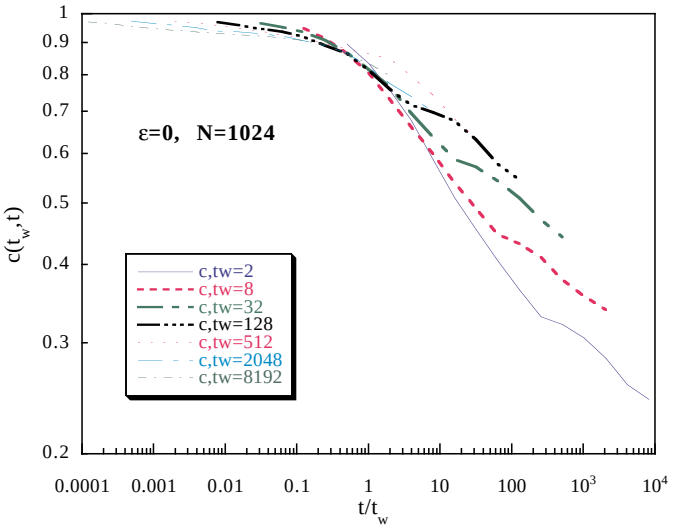

Figure 3. As in figure 2, but versus t/t_w.

(This figure can be viewed in colour in the electronic version of the article; see `http://www.iop.org`)

small values of t_w the system decays fast, and the decay rate slows down when one looks at high values of t_w.

Here we are in the same situation as in [16] for the simulations of the hypercubic model: on the observed timescales $q^2(t)$ (as measured from two copies of the system in the same noise realization) stays small ($\leqslant 0.04$). The system has not crossed the very high barriers that was encountered on the way. We will discuss that in more detail in the following sections, together with the fact that the energy is decaying to its asymptotic value with a very good power law (at $\epsilon = 0$ and $N = 1024$ the exponent is of order 0.4).

In figure 3 we plot the same data as a function of t/t_w (again on a double log scale). This is the usual search for an aging-like scaling. Here the scaling of the data is reasonable but obviously not perfect: scaling violations are clearly present, but a detailed study of this phenomenon is beyond the scope of this study. The plateau (to be) for $t < t_w$ is connected to the value of the same state overlap q_{EA}† (see [17] and figures 3–5 of [18]). We remark that these results are compatible with those obtained by Rossetti [19] on very large lattices (SK model up to $N = 8192$) and (when looking in details at the graphs: the aging curves tend to separate soon after the crossing point for all values of t_w) with the ones obtained by Cugliandolo *et al* [16] on the alternative, hypercubic definition of the mean field. We just repeat that violations of a perfect aging scaling are quite clear here. Definitely the usual SK model does not show any easily explainable form of scaling.

We will now try to analyse what happens in the non-Hamiltonian dynamics. We start with the non-Hamiltonian dynamics by looking at a large perturbation: we use $\epsilon = 0.4$, 20 samples and $N = 1024$. In figure 4 the correlation functions for different values of t_w (here on a simple linear–linear scale). It is clear that things are now very different. The decay at very small waiting times is faster than for larger t_w, but already for $t_w \leqslant 32$ there is very little dependence of c over t_w. The curves from different t_w are collapsing on a same

† We thank Juan Ruiz-Lorenzo for an interesting conversation on this subject.

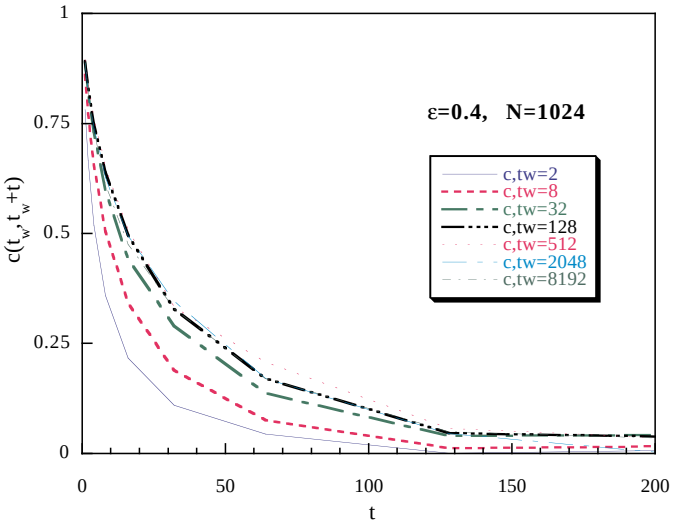

Figure 4. As in figure 2, but $\epsilon = 0.4$, and it is plotted on a linear–linear scale.
(This figure can be viewed in colour in the electronic version of the article; see `http://www.iop.org`)

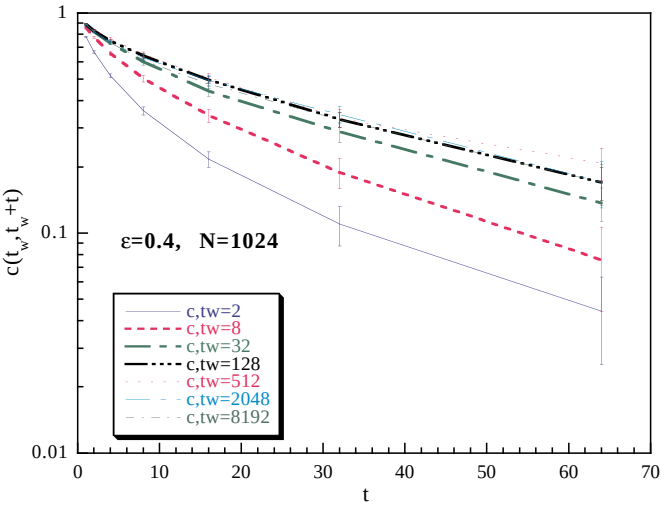

Figure 5. As in figure 2, but $\epsilon = 0.4$, and it is plotted on a linear–log scale.
(This figure can be viewed in colour in the electronic version of the article; see `http://www.iop.org`)

universal decay curve.

Since we are (maybe) expecting here an exponential decay of the time-dependent correlations (but we will see this is a far from evident fact) we plot in figure 5 the correlation functions for different values of t_w on a linear–log scale. Here we also include the error from sample-to-sample fluctuations. The lines would be asymptotically straight lines in case of an asymptotic exponential decay. The reader can start to observe that in this case

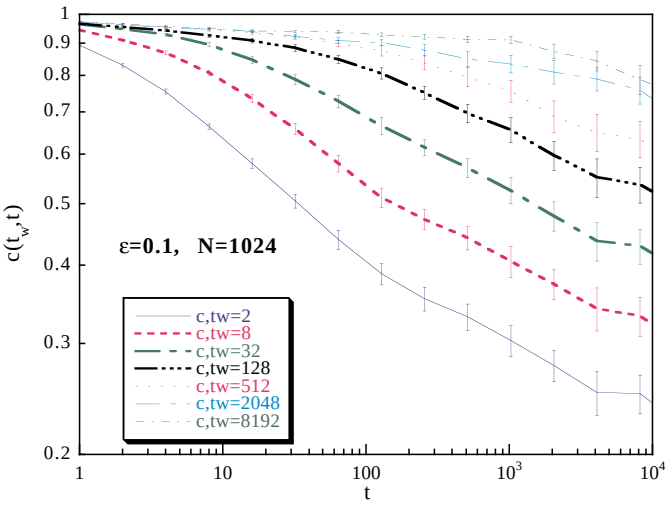

Figure 6. As in figure 2, but $\epsilon = 0.1$.

(This figure can be viewed in colour in the electronic version of the article; see http://www.iop.org)

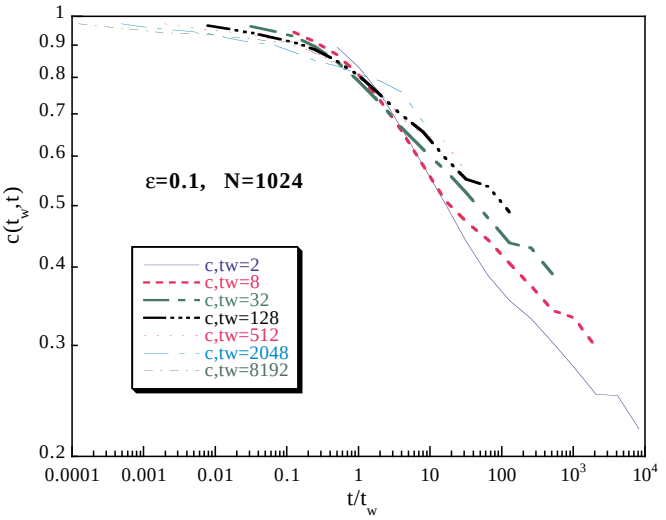

Figure 7. As in figure 3, but $\epsilon = 0.1$.

(This figure can be viewed in colour in the electronic version of the article; see http://www.iop.org)

($\epsilon = 0.4$) in all the time range where we can determine an *effective* t-dependent correlation time $\tau_e(t)$ (by looking, for example at the local gradient of the logarithm of the correlation function), such $\tau_e(t)$ is increasing (i.e. the curves are bending up in the whole region where we have been able to determine them with good statistical precision).

Other data for ϵ going from 0.3 to 0.5 give very similar suggestions. Our first conclusion can be reached at this point: systems with large non-Hamiltonian perturbations do indeed have a quite different, typically non-aging, dynamical behaviour, but one has to be careful

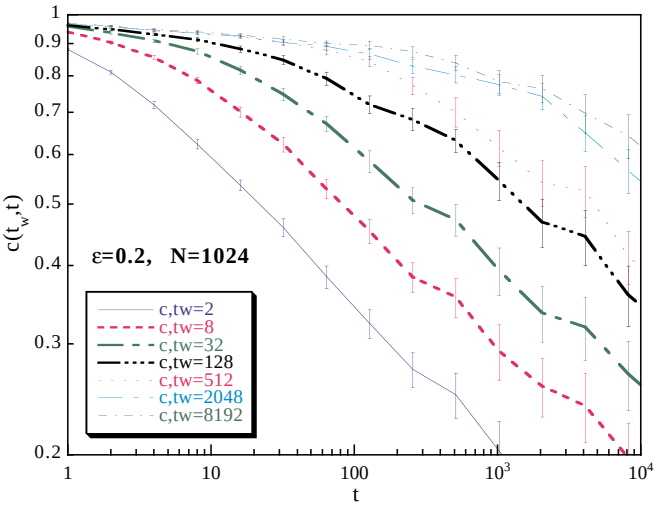

Figure 8. As in figure 2, but $\epsilon = 0.2$.

(This figure can be viewed in colour in the electronic version of the article; see `http://www.iop.org`)

since it looks difficult to pinpoint a real exponential decay.

Let us now turn to a reasonably small value of the non-Hamiltonian perturbation. We select $\epsilon = 0.1$, that is not too small: the non-symmetric couplings are coupled with a strength 0.1 times β while the symmetric couplings interact with a strength of 0.9. These data turn out indeed to be dramatically similar to the ones at $\epsilon = 0$. Figures 6 and 7 are analogous to figures 2 and 3; the similarity is self-explanatory. Later we will try to quantify the differences and to elucidate their meaning. By now we observe that for large lattices ($N = 1024$ for the infinite-range model is a large lattice, since one has 1 000 000 couplings) and long times (we follow the system up to t and t_w of order 16 384) the model with $\epsilon = 0.1$ shows an aging behaviour as good as the one observed for the pure SK model.

Before discussing a more quantitative analysis of these data, we shall state a few comments about an intermediate case, $\epsilon = 0.2$. Here the pattern of $c(t_w, t_w + t)$ is different from both the usual aging case (like the one we find for $\epsilon = 0.0, 0.1$) and the typical fast decay to an equilibrated state (see $\epsilon = 0.4$, even if we will see that even here things are more complex).

In figure 8 the correlation function is a function of t. The pattern is reminiscent of an aging pattern, even if for large t_w the situation is not so clear. The plot of c versus t/t_w in figure 9 is more innovative: here the typical crossing one expects at $t/t_w \simeq 1$ is moved to larger values of t/t_w, which increase with t_w. The scaling is different from the one in the Hamiltonian case.

It is interesting to note, as a basis of the discussion we will present in one of the next paragraphs, that this is not only an effect we detect at high t_w values. Already for very short t_w (figures 2 and 8, for example) we find a crossing at t of order 10. We also want to notice that, looking at their value, in the region $t > t_w$ the $\epsilon = 0.2$ data seem to show a better pure t/t_w scaling than the pure ones: but this is probably not a very relevant feature (that could be typical of a transient behaviour).

The similarity of the correlation functions in the pure SK model and the ones in the model with $\epsilon = 0.1$ calls for a better scrutiny. The very remarkable similarity of the two

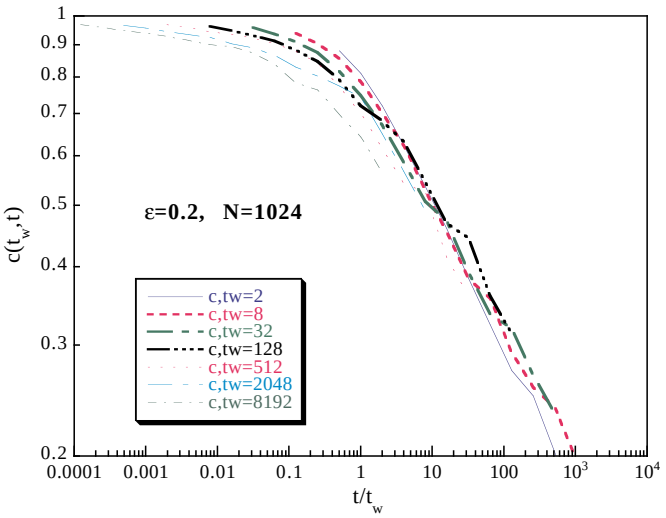

Figure 9. As in figure 3, but $\epsilon = 0.2$.

(This figure can be viewed in colour in the electronic version of the article; see http://www.iop.org)

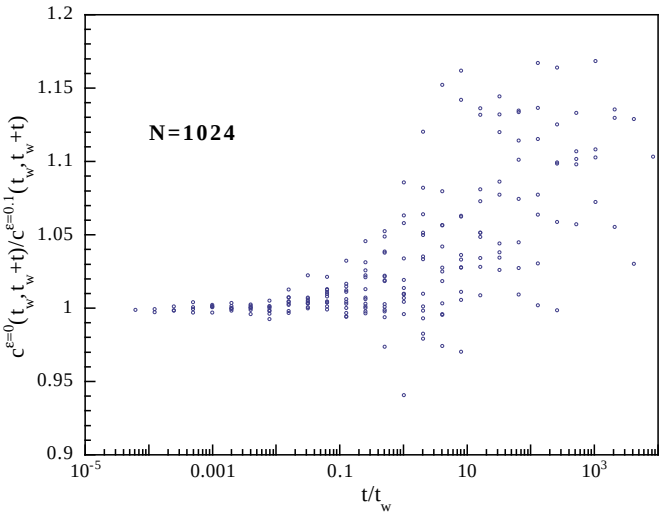

Figure 10. The ratios of $c(t_w, t_w + t)$ at the same t and t_w with $\epsilon = 0$ and $\epsilon = 0.1$ versus t/t_w on a linear–log scale.

(This figure can be viewed in colour in the electronic version of the article; see http://www.iop.org)

sets of functions has to be quantified in some way. In order to do that we compute the ratios of the correlation functions at the same t and t_w with $\epsilon = 0$ and $\epsilon = 0.1$, and we plot them in figure 10. The correlation functions are indeed very similar, but for increasing values of t/t_w we start to see a small difference (typically the higher points at fixed t/t_w are for higher t values). We do not plot the statistical errors, which would blur the plot in an extreme manner, but even if any individual ratio is compatible with one, the large time

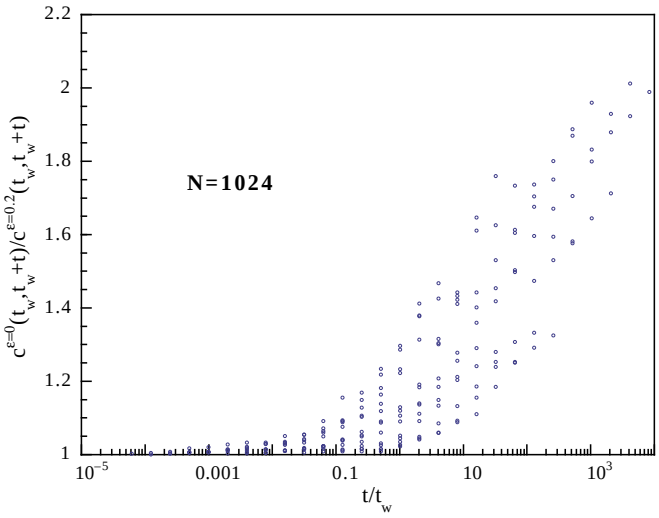

Figure 11. As in figure 10, but $\epsilon = 0$ over $\epsilon = 0.2$.

(This figure can be viewed in colour in the electronic version of the article; see `http://www.iop.org`)

growth of the ratios is clear and statistically significant: at large times the correlations for the $\epsilon = 0.1$ case start to decrease faster than for the pure SK case. It is a very small effect, and its meaning is not unambiguous: it could signify that we are exiting a transient phase and aging is ending, or it could just be an irrelevant renormalization (a shift of the effective temperature of the system). But the effect is clear, and we note it here.

In figure 11 we plot the same ratio, but here the $\epsilon = 0$ value is divided times the $\epsilon = 0.2$ value. Note that the vertical scales of this and the former plots are very different. Here the faster decay of the non-Hamiltonian case is very clear: for t/t_w of order 10^4 the ratio is of order two.

Two remarks: first the departure from a ratio close to unit comes for the $\epsilon = 0.1$ case quite late. The departure from unit is far more pristine at $\epsilon = 0.2$. For example, one can notice that a value of 1.05 is reached at $t/t_w \simeq 10$ in the first case, and of order $10^{-3} - 10^{-2}$ in the second case.

If one tries using, in this way, a very qualitative definition of an ϵ-dependent correlation time one obtains a divergence that is faster than the one obtainable with an ϵ^{-6} scaling (see later). It should also be noticed that this effect is not dominated by finite size effects: on different volumes we get very similar results.

The next natural thing to do is to check for correlation times. The Crisanti–Sompolinsky [1, 2] result for the spherical model suggest a behaviour

$$\tau \simeq \epsilon^{-6} \tag{20}$$

and one can proceed by trying to support or falsify this expectation. In this case one would start from the larger ϵ values, where the asymptotic decay looks better exposed, and try to go down to lower ϵ values.

Determining correlation times is typically not as easy as one expects. The main caveat is indeed that in a numerical simulation at best one can establish upper bounds on correlation times: correlation times that are larger than the simulation time cannot be detected. In the case of systems which exhibit (or could exhibit) an aging behaviour things are even more

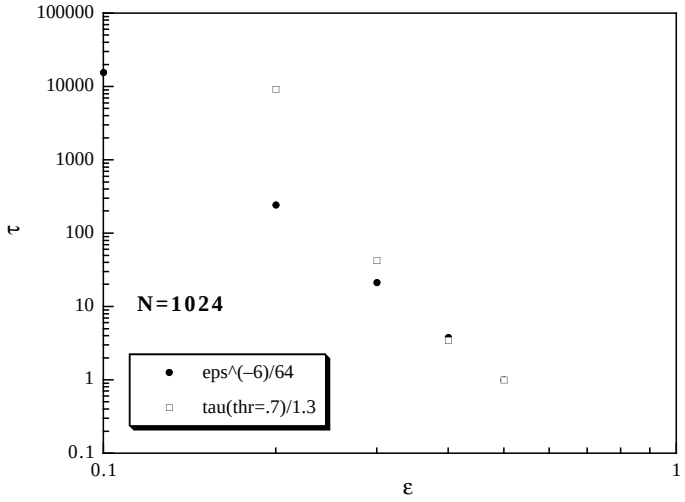

Figure 12. We plot the time needed from c to reach the value 0.7, and ϵ^{-6}. As a function of ϵ, on a double log scale.

complex since *a priori* one cannot average over t_w. Only after checking that we are in a region of time translational invariance are we allowed to average over different waiting times.

The first, easy approach, consists of defining the correlation time as the time after which the time-dependent correlation function reaches, down from 1, a given value, say $\tilde{c}$. In figure 12 we plot the time needed for c to reach the value of 0.7, and ϵ^{-6} as a function of ϵ (we have also done the same analysis for $\tilde{c} = 0.5$). It would be incorrect to average over t_w's: only *a posteriori*, after checking that we are in an asymptotic region of a simple phase where time-translational invariance holds, would that be justified. We have checked indeed that doing that can lead to a false scaling. In figure 12 we have only used the largest t_w points available to us ($t_w = 2^{14}$). We have normalized the data in the plot such that the data points coincide at the higher ϵ value ($\epsilon = 0.5$). It is clear that already at $\epsilon = 0.3$ the ϵ^{-6} scaling does not hold (we are using a double log scale!). At $\epsilon = 0.2$ the discrepancy from an ϵ^{-6} scaling is severe, and for $\epsilon = 0.1$ we cannot determine τ since the correlation function with $t_w = 2^{14}$ does not reach the value of 0.7. Anyhow, here τ would be so large to be completely incompatible with an ϵ^{-6} scaling.

When using a lower threshold (that should not underestimate the true correlation time so much) the situation is even more dramatic. In this case we can only determine τ for $\epsilon \geqslant 0.3$, and the deviation from an ϵ^{-6} scaling is more severe.

From this, very naive analysis, we can already conclude that if we could define a correlation time τ for $\epsilon \to 0$ it would be growing far more dramatically than ϵ^{-6}. The analysis of section VI.A in [2] is in this sense probably incorrect since the authors average the correlation function over small t_w values (but they were not working in identical conditions to us, both because of the exact form of the non-Hamiltonian contribution to the force and since they were at $T = 0.5$).

Since the question of correlation times, of their scaling behaviour and of the functional form of the time-dependent correlation functions of the non-Hamiltonian system, is of crucial interest, we have decided to perform a careful analysis of this issue. The standard approach for trying to expose clearly an asymptotic exponential behaviour is based on the definition

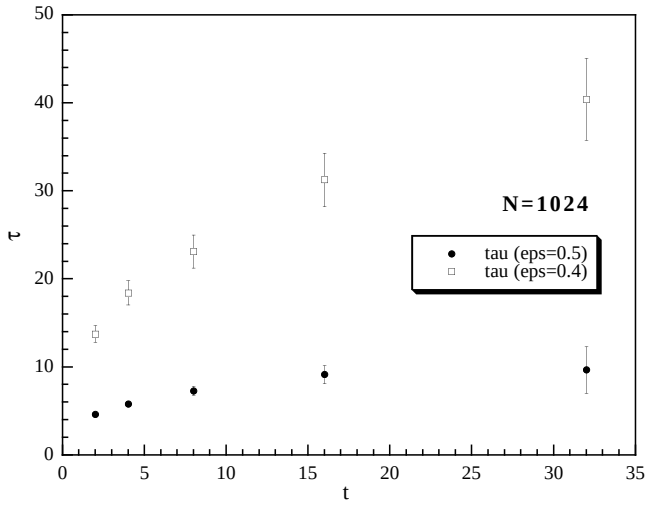

Figure 13. $\tau_{\rm eff}(t)$ versus t for $\epsilon = 0.5$ and 0.4.

of a time-dependent effective correlation time $\tau_{\rm eff}(t)$. If we are in the asymptotic large time regime of a phase with an exponential decay of time-dependent correlation functions

$$c(t) \simeq A{\rm e}^{-\frac{t}{\tau}} \tag{21}$$

and

$$\tau_{\rm eff}(t) \equiv \left(\frac{1}{t}\log\left(\frac{c(t)}{c(2t)}\right)\right)^{-1} = \tau \tag{22}$$

$\tau_{\rm eff}(t) \to \tau$ at large times.

We have hinted before that already figure 5 suggests that we cannot, from the data from our numerical simulations, exhibit a clean exponential behaviour even at $\epsilon = 0.4$. In figure 13 we plot $\tau_{\rm eff}(t)$ versus t for $\epsilon = 0.5$ and 0.4.

We have averaged curves for different t_w in the region where the dependence over t_w is smaller than the statistical error (16 for $\epsilon = 0.5$, 64 for $\epsilon = 0.4$, 512 for $\epsilon = 0.3$, 2048 for $\epsilon = 0.2$, while for $\epsilon = 0.1$, 0.0 we have only selected the largest t_w). We plot the larger ϵ values since for lower ϵ it is quite clear that we are not observing an exponential decay at all. But, as we said, already for large ϵ the effective correlation time steadily increases, as a function of t, in the time region we can handle safely. It is not clear from our data whether $\tau_{\rm eff}(t)$ is reaching a plateau, but it is clear that where we can determine it with good precision it has not reached an asymptotic value.

We have also tried global fits to an exponential decay, by changing the number of data points used in the fit. They are quite bad for all ϵ values (but maybe at $\epsilon = 0.5$ where the noise threshold is reached after only a few data points). If discarding enough points close to the origin maybe an exponential fit is preferred at $\epsilon = 0.5$ and 0.4, while a power fit is preferred at $\epsilon = 0.3$. For lower ϵ values one cannot find a simple behaviour that fits the data well.

The evidence presented in this section does not completely clarify the main issue. On the timescales we can observe that there is still aging for small non-Hamiltonian perturbations, while for large perturbations aging disappears. Still, even in the case of large perturbations a pure exponential behaviour is slow to emerge. Somehow it is clear that we are dealing

with a system with a very complex dynamics, even if it is difficult to establish whether we are dealing with a transient behaviour or with an asymptotic effect. But complexity is strong, and manifests itself with different signatures that we have discussed in some details, in all the parameter range we have explored. If we try to define a correlation time, even where it is not clear we could define one, it turns out to diverge faster than a spherical spin model analogy would predict. That could be connected to a signature of the replica symmetry breaking pattern of the Parisi solution.

Maybe the most important question we are not able to answer in a precise way is: is something drastic happening when going from large non-Hamiltonian perturbations (where we know that we will eventually get a non-aging behaviour) to small perturbations? It is very difficult to discriminate between a transient behaviour on a very long timescale and a true asymptotic behaviour. If any, our feeling about this issue is that yes, things at $\epsilon = 0.1$ are different from things at $\epsilon \geqslant 0.2$. This is based both on the scaling of $\tau(\epsilon)$ that we have discussed before (that is not compatible even with the very high power predicted by the spherical spin model solution), and by a hand-waving argument we give now. Let us be very conservative and say that $\tau(\epsilon = 0.2)$ is of order 300 (this is by far a lower bound, and τ is probably, if any, far larger than that), and $\tau(\epsilon = 0.1) > 10\,000$ (this is obvious). At $\epsilon = 0.1$ for all times in our measurement windows ($O(2^{14})$) we see a very good aging. We would expect that at $\epsilon = 0.2$, at least for $t \ll 300$, we should have a transient aging, that could die out later on. We do not have that at all. Already at $t_w = 2, 4$ aging curves at $\epsilon = 0.2$ behave in a way that is dramatically different to usual aging. The argument of the transient behaviour was used in [1] to describe the situation at finite ϵ, and it surely works for the spherical spin model: but here we have evidence that the argument does not apply. Because of that, the wrong scaling and the further evidence we will present in the next section we cannot exclude that something changes at a critical value of ϵ.

5. Power laws

Slow relaxation towards thermal equilibrium expectation values is one of the typical signatures of disordered systems. First, Gardner *et al* [20] have pointed out and quantified this kind of effect in spin glasses. Eisfeller and Opper [21] have introduced a powerful dynamical functional method that allows us to compute with good precision the power exponents at $T = 0$. Ferraro [22] has generalized this work to $T \neq 0$. Work based on numerical simulations [19, 23, 24] has made these computations detailed: one can determine with a reasonable accuracy power exponents even at $T \neq 0$, both for the remnant magnetization and for the energy decay.

We have used the decay towards equilibrium of typical observable quantities (such as the internal energy $E(t)$ and the squared overlap $q^2(t)$) as a probe of the existence of a complex behaviour even for the non-Hamiltonian, $\epsilon \neq 0$ case. We have measured and tried to fit the time-dependent internal energy

$$E(t) \simeq E_\infty + At^{-\eta} \tag{23}$$

and have analysed the slow growth of $q^2(t)$ towards its equilibrium value. On general grounds we notice that the exponents we have determined for the energy are quite stable: they do not seem to depend much on the lattice size (we have checked different sizes) and over the time window we use to fit them.

First we present the results from our runs at $T = 0.2$, the same as we discussed in the former section of this note. We start from $E(t)$. At $\epsilon = 0.0$ and $\epsilon = 0.1$ a power fit is perfect, while an exponential decay is clearly ruled out. In figure 14 we plot the data with

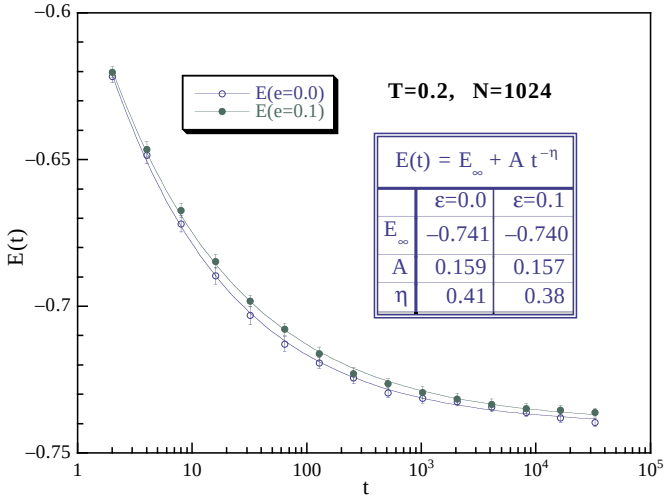

Figure 14. $E(t)$ versus t (linear–log scale) for $\epsilon = 0.0$ and 0.1. $N = 1024$, $T = 0.2$. The lines are for the best power fits.

(This figure can be viewed in colour in the electronic version of the article; see http://www.iop.org)

the best fits for $\epsilon = 0.0$ and $\epsilon = 0.1$. The error here is of 1–3 on the last digit. It is clear that the two sets of data are compatible in the statistical error: a small shift in the effective temperature of the system is the best way to explain the small shift in the data (the situation will be similar for higher T values). Also at $\epsilon = 0.2$ and 0.3 we get a perfect power fit, with an exponent of 0.39 and 0.48 respectively, and an exponential behaviour is ruled out. $\epsilon = 0.4$ is an intermediate case, where both a power fit (that would give an exponent of 0.63) and an exponential fit are not very good. At $\epsilon = 0.5$ the exponential fit is definitely better, and the energy clearly reaches its asymptotic value.

For zero and small ϵ we only see the very slow growth of $q^2(t)$, that is very far from its asymptotic value. At $\epsilon = 0.0$ and $\epsilon = 0.1$ the slow growth is compatible with a logarithmic behaviour. For higher ϵ values one starts to see $q^2(t)$ approaching an asymptotic value, but in this case, even when the asymptotic value is very clear, a power fit does not work well. It is interesting to notice that somehow the functional form of the time dependence of $q^2(t)$ is very different from the one of the energy $E(t)$, where the power law is very clear. As we will also show for $T = 0.5$ with figure 16 the best way to describe the behaviour of $q^2(t)$ would be by a very slow logarithmic growth that stops abruptly after reaching its finite volume asymptotic value.

We have also studied the system at higher $T = 0.5$ and smaller volume $N = 256$, by running longer simulations (10^6 steps, and 10 samples for each ϵ value). That has been done in order to reach equilibrium at $\epsilon = 0.0$ and for a comparison with finite ϵ (to check, for example, if the finite ϵ system converges to an effective stable Boltzmann-like probability distribution, see (6)). The situation is very similar to the case of $T = 0.2$, the difference being that here the energy and the q^2 plateau's are very clear already at $\epsilon = 0.0$ (equilibrium for both energy and q^2 are apparently reached after O(10^3) steps), and the exponents of the power decay are higher (since we are at higher T). In figure 15 we show $E(t)$ at $\epsilon = 0.0$ and 0.1 with the best power fit (errors are up to O(5) on the last digit). Again the results are very similar, and the power fit is very good. An exponential fit is not able to describe the

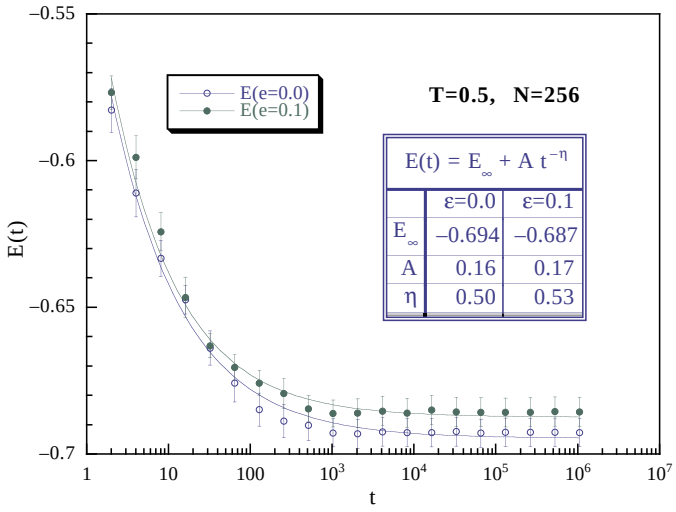

Figure 15. $E(t)$ versus t (linear–log scale) for $\epsilon = 0.0$ and 0.1. $N = 256$, $T = 0.5$. The lines are for the best power fits.

(This figure can be viewed in colour in the electronic version of the article; see `http://www.iop.org`)

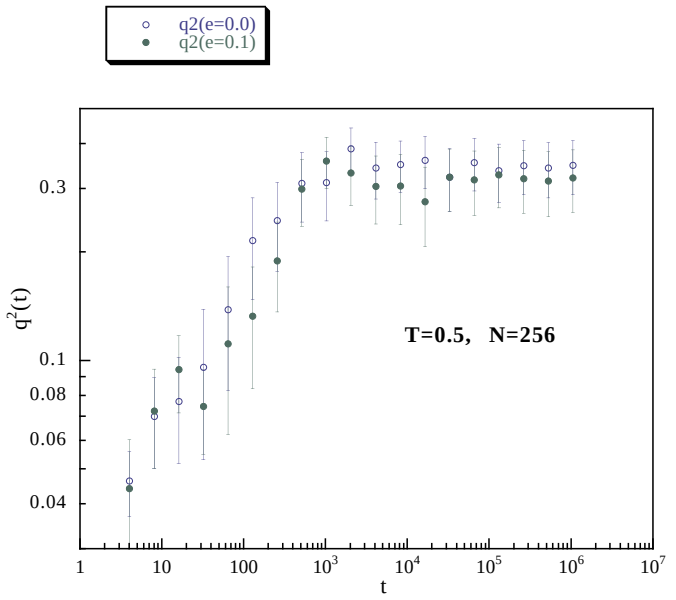

Figure 16. $q^2(t)$ versus t (linear–log scale) for $\epsilon = 0.0$ and 0.1. $N = 256$, $T = 0.5$.

data. Here, already at $\epsilon = 0.2$ convergence to equilibrium is very fast and an exponential fit works reasonably. At $\epsilon = 0.4$ the best exponent of the power fit is close to one. At $\epsilon = 0.5$ the exponential fit is perfect.

$q^2(t)$ converges to a clear plateau, but as we said before it is difficult to find a correct functional form to describe such time dependence. In figure 16 we show $q^2(t)$ at $\epsilon = 0.0$

and 0.1, where a power fit does not work well. The situation is qualitatively very similar at higher ϵ values, but $q^2(t)$ reaches lower plateau values. At $\epsilon = 0.4$ the asymptotic value of q^2 is very small. At $\epsilon = 0.5$ the asymptotic value of q^2 is 0.02, i.e. fully compatible with zero.

Therefore, slow convergence to equilibrium is clear for different values of $T < T_c^{(\epsilon=0.0)}$. We can never see, in the time ranges we investigate, any significant difference when going from $\epsilon = 0.0$ to $\epsilon = 0.1$. It also has to be noticed that in the case where we reach thermal equilibrium for ϵ not too large the expectation value of q^2 at equilibrium is far larger than a pure finite size contamination: for $N = 256$ $\langle q^2 \rangle$ is clearly non-zero in a large ϵ range. In the next section we will try to understand if this is a finite size effect or not.

6. Equilibrium

In the former two sections we have analysed the dynamical properties of the non-Hamiltonian dynamics. In this section we have taken the complementary point of view and, by studying small lattices on longer timescales we have investigated the equilibrium properties of the model. Even if the model is not defined from a Hamiltonian we can define its equilibrium properties from the large time limit of the dynamics. We have measured the probability distribution of the overlap $P(q)$, and compared the SK model with the non-Hamiltonian dynamics. We have systematically analysed the dependence of the equilibrium properties from the finite volume (up to the largest volume on which we have been able to thermalize the system, see later).

We have worked at $T = 0.5$, running 10^6 full sweeps of the lattice and using the second two thirds of the sweeps for measuring equilibrium properties. We have selected, as before, ϵ going from 0 to 0.5 with increments of 0.1.

We have used $N = 64$, 128 and 256 (respectively with 20, 10 and 10 samples for each ϵ value). In all case we have checked that all the relevant observable quantities (for example $E(t)$, $q^2(t)$) have reached a very clear plateau, where they are stable in all of the measurement region. We have also analysed directly the sample-dependent probability distributions $P_J(q)$ checking the symmetry sample-by-sample (a very strong check). At $\epsilon = 0$, where the thermalization is more difficult, the $P_J(q)$ is very symmetric at $V = 64$ on all samples. At $V = 128$ there is again a very good symmetry (the maximum discrepancy is of the order of 25% of the double peak height. At $V = 256$ some of the samples have quite an asymmetric $P(q)$, but for all 10 systems it looks very plausible that true equilibrium has been reached: the average $P(q)$ is nicely symmetric. We would not have succeeded to thermalize larger systems.

In figures 17–19 we plot $P(q)$ for different ϵ and N values (always at $T = 0.5$). It is clear that the double peak structure of the Parisi broken phase of the SK model, and that for high ϵ values, one obtains a trivial distribution centred around $q = 0$.

It is more interesting to follow, for example, the $\epsilon = 0.3$ case as a function of N. Here from a (already quite soft) double peak structure at $N = 64$ one goes to a broad peak around $q = 0$ at $N = 256$. At $\epsilon = 0.2$ there is the same kind of effect: a strong double peak at $N = 64$ softens at $N = 128$. At $N = 256$ we are left with a flat plateau including q values going from -0.5 to 0.5.

In the case $\epsilon = 0.1$ once again we get results that are very similar to the ones we get for the pure SK model. In our N range we cannot observe any systematic effect.

To make this point clearer, in figure 20 we plot the ratio of the $P(q)$ for the $\epsilon = 0.1$ model and the pure SK model as a function of q, for the three N values that we have analysed. Apart from large fluctuations we cannot see any systematic trend. For small q

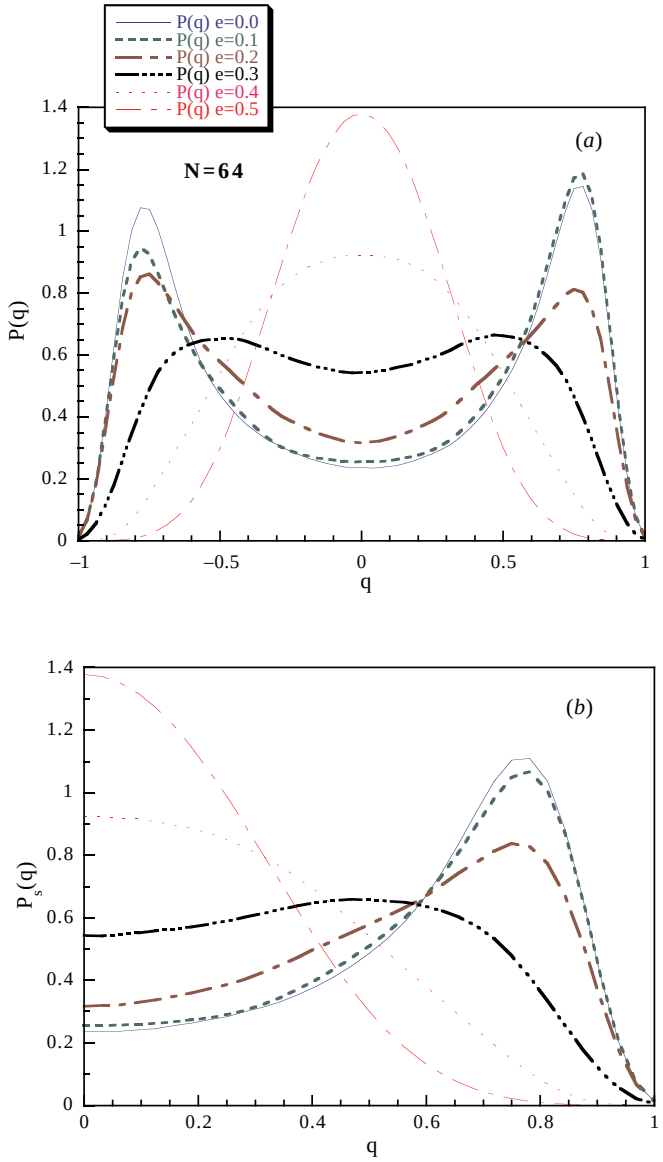

Figure 17. $P(q)$ versus q for different ϵ values, $N = 64$. In (a) the full $P(q)$ curve shows where the quality of the symmetry under $q \to -q$ gives a measure of how good our thermalization was. (b) shows the symmetrized $P_s(q)$.

(This figure can be viewed in colour in the electronic version of the article; see `http://www.iop.org`)

on the large lattice we have a quite large ratio, but the statistical undetermination is large in this case.

In this section we have been exploring features of the model that are different from the dynamical issues we were discussing before. Here we are discussing equilibrium properties: the system could very well have a complex dynamics on divergent timescales but a trivial large time limit. Still, what we find is that again, on the volume scales we are able to

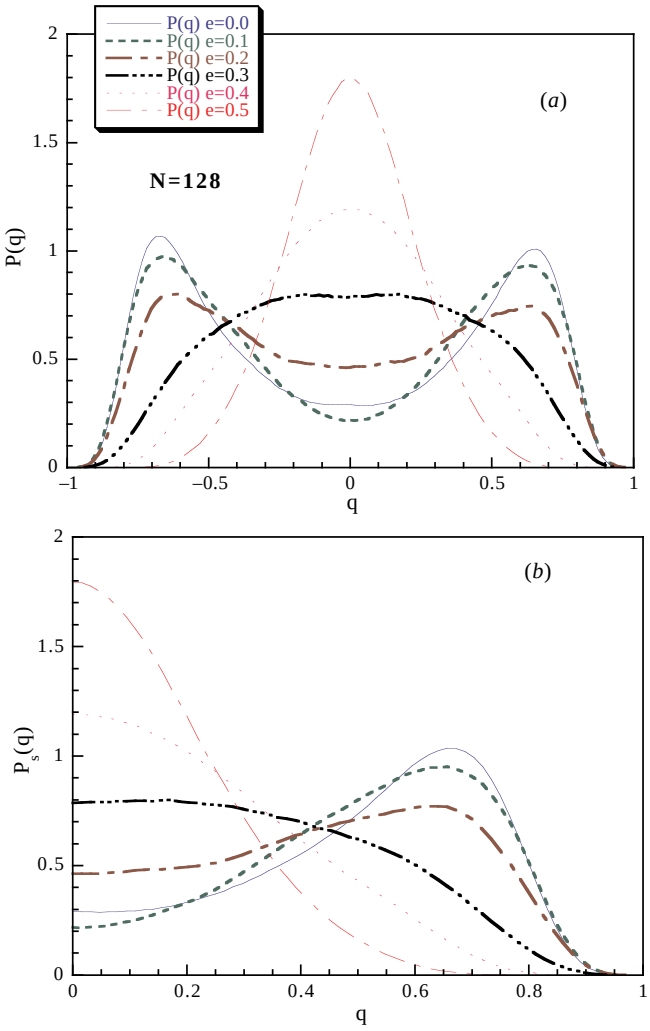

Figure 18. As in figure 17 but $N = 128$.

(This figure can be viewed in colour in the electronic version of the article; see http://www.iop.org)

disentangle numerically, there is no difference among the SK model and the one with a small non-Hamiltonian perturbation. Also we notice that, at least for large perturbations, the small lattices fake a non-trivial structure that disappears in the infinite volume limit. The same effect could make trivial the theory with small perturbations on very large volume, but here we cannot see such an effect.

7. Conclusions

Our numerical simulations surely show that the non-Hamiltonian systems we have studied have a very interesting, complex behaviour, and show that the spherical spin model analogy is probably not all of the story.

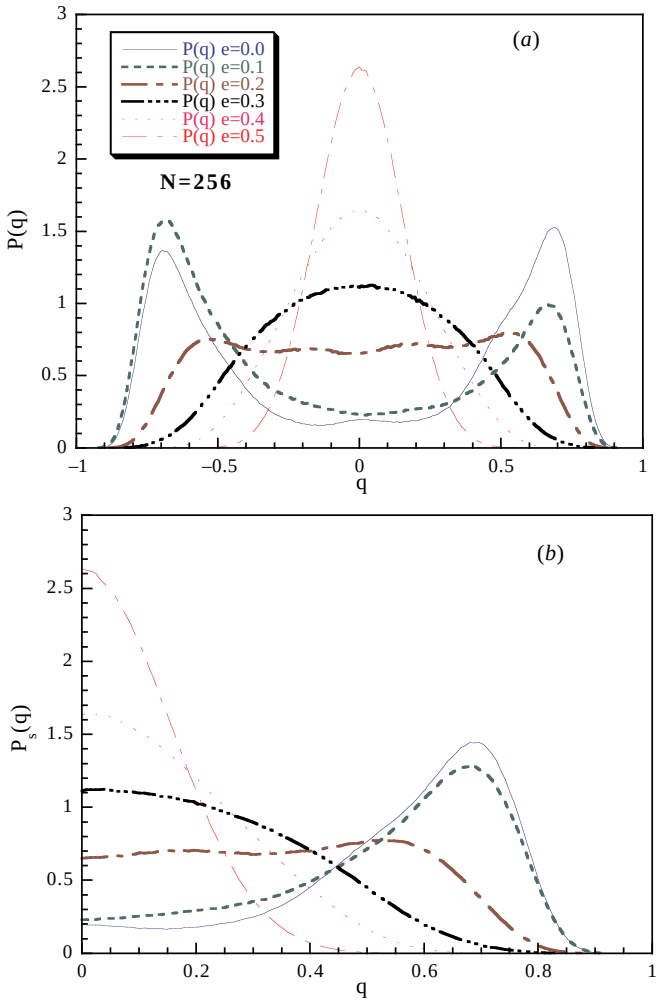

Figure 19. As in figure 17 but $N = 256$.

(This figure can be viewed in colour in the electronic version of the article; see `http://www.iop.org`)

We have studied aging. We have found that on the timescales we could investigate (that are, one should not forget, of the order of the largest timescales that have been used to claim numerically that the pure model undergoes aging) systems with small perturbations age, while systems with a large non-Hamiltonian term have a conventional behaviour (with some care to be used when discussing the intermediate ϵ case, $\epsilon = 0.2$ for us). Our data do not look compatible with the ϵ^{-6} scaling one finds for the spherical spin model [1, 2]. Also the aging systems look different from the non-aging ones on all timescales, making the possibility of a transient behaviour less favoured.

We have studied the time dependence of observables such as the internal energy $E(t)$ or $q^2(t)$. We have found clear power law decays for small perturbations.

Finally, we have studied equilibrium. Here we are looking at a regime that is very different from the previously discussed one. Here we have also seen that for small

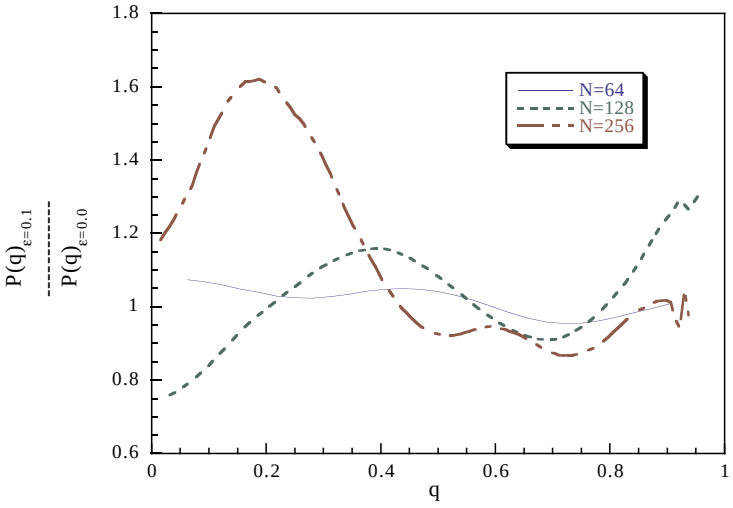

Figure 20. The ratio of $P(q)$ at $\epsilon = 0.0$ and $\epsilon = 0.1$ as a function of q, for different N values. (This figure can be viewed in colour in the electronic version of the article; see `http://www.iop.org`)

perturbations one finds results that are very similar to the ones of the pure model, but we have also seen that for larger ϵ small lattices do produce fake double peak structures in the probability distribution of the overlap.

There is room, as is often the case, for more analytical and numerical work.

Acknowledgments

We warmly thank David Dean and Daniel Stariolo for many useful discussions on the subject. We are indebted to Leticia Cugliandolo and Jorge Kurchan for informing us about the results of [12] prior to publication, and for a very explicative and helpful conversation. We acknowledge useful conversations with Giorgio Parisi, Paola Ranieri and Juan Ruiz-Lorenzo.

References

[1] Crisanti A and Sompolinsky H 1987 Dynamics of spin systems with randomly asymmetric bonds: Langevin dynamics and a spherical model *Phys. Rev.* A **36** 4922

[2] Crisanti A and Sompolinsky H 1988 Dynamics of spin systems with randomly asymmetric bonds: Ising spins and Glauber dynamics *Phys. Rev.* A **37** 4865

[3] Hertz J, Grinstein G and Solla S 1986 *Neural Networks for Computing (AIP Conf. Proc. 151)* ed J Denker, p 213

[4] Parisi G 1986 Asymmetric neural networks and the process of learning *J. Phys. A: Math. Gen.* **19** L675.

[5] Rieger H, Schreckenberg M and Zittartz J 1989 Glauber dynamics of the asymmetric SK-model *Z. Phys.* B **74** 527

[6] Schreckenberg M 1992 Attractors in the fully asymmetric SK-model *Z. Phys.* B **86** 453

[7] Pfenning T, Rieger H and Schreckenberg M 1991 Numerical investigation of the asymmetric SK-model with deterministic dynamics *J. Physique* I **1** 323

[8] Schreckenberg M and Rieger H 1992 Remanence effects in symmetric and asymmetric spin glass models *Z. Phys.* B **86** 443

[9] Eisfeller H and Opper M 1994 Mean-field Monte Carlo approach to the Sherrington–Kirkpatrick model with asymmetric couplings *Phys. Rev.* E **50** 709
[10] Nützel K and Krey U 1993 Subtle dynamic behaviour of finite-size SK spin glasses with non-symmetric couplings *J. Phys. A: Math. Gen.* **26** L591
[11] de Almeida R M C, Bernardi L and Campbell I A 1995 Damage spreading in $\pm J$ asymmetric Ising spin glasses *J. Physique* I **5** 355
[12] Cugliandolo L F, Kurchan J, Le Doussal P and Peliti L 1996 Glassy behaviour in disordered systems with non-relaxational dynamics *Preprint* cond-mat/9606060
[13] Sompolinsky H and Zippelius A 1982 *Phys. Rev.* B **25** 6860
[14] Cugliandolo L F and Kurchan J 1993 *Phys. Rev. Lett.* **71** 173
[15] For a recent review see Rieger H 1995 Monte Carlo studies of ising spin glasses and random field systems *Annual Reviews of Computational Physics* ed D Stauffer (Singapore: World Scientific)
[16] Cugliandolo L, Kurchan J and Ritort F 1994 Evidence of aging in spin glass mean-field models *Phys. Rev.* B **49** 6331
[17] Mezard M, Parisi G and Virasoro M 1987 *Spin Glass Theory and Beyond* (Singapore: World Scientific)
[18] Parisi G, Ricci Tersenghi F and Ruiz-Lorenzo J 1996 Equilibrium and off-equilibrium simulations of the 4*d* gaussian spin glass *Preprint* cond-mat/9606051
[19] Rossetti D 1995 *Comportamento Dinamico del Modello di Campo Medio dei Vetri di Spin* Tesi di Laurea, Università di Roma, La Sapienza unpublished
[20] Gardner E, Derrida B and Mottishaw P 1987 *J. Physique* **48** 741
[21] Eisfeller H and Opper M 1992 *Phys. Rev. Lett.* **68** 2094
[22] Ferraro G 1994 *Preprint* cond-mat/9407091
[23] Baldassarri A 1996 Non-equilibrium Monte Carlo dynamics of the Sherrington–Kirkpatrick mean field spin glass model *Preprint* cond-mat/9607162
[24] Baillie C, Johnston D, Marinari E and Naitza C 1996 *J. Phys. A: Math. Gen.* **29** 6683